Chinese Society of Aeronautics and Astronautics
& Beihang University

Chinese Journal of Aeronautics

cja@buaa.edu.cn
www.sciencedirect.com

Theoretical investigation of shock stand-off distance for non-equilibrium flows over spheres

Hua SHEN [a], Chih-Yung WEN [b],*

[a] *Extreme Computing Research Center, Computer Electrical and Mathematical Science and Engineering Division, King Abdullah University of Science and Technology, Thuwal 23955-6900, Saudi Arabia*
[b] *Department of Mechanical Engineering, The Hong Kong Polytechnic University, Kowloon 999077, Hong Kong Special Administrative Region, China*

Abstract   We derived a theoretical solution of the shock stand-off distance for a non-equilibrium flow over spheres based on Wen and Hornung's solution and Olivier's solution. Compared with previous approaches, the main advantage of the present approach is allowing an analytic solution without involving any semi-empirical parameter for the whole non-equilibrium flow regimes. The effects of some important physical quantities therefore can be fully revealed via the analytic solution. By combining the current solution with Ideal Dissociating Gas (IDG) model, we investigate the effects of free stream kinetic energy and free stream dissociation level (which can be very different between different facilities) on the shock stand-off distance.

© 2018 Chinese Society of Aeronautics and Astronautics. Production and hosting by Elsevier Ltd. This is an open access article under the CC BY-NC-ND license (http://creativecommons.org/licenses/by-nc-nd/4.0/).

1. Introduction

When a supersonic/hypersonic flow over a blunt body like a sphere, a detached bow shock forms around the body, and the level of the non-equilibrium of the flow is measured by the following dimensionless reaction rate parameter,[1] $\Omega \equiv \left(\frac{d\alpha}{dt}\right)_s \frac{D}{2u_\infty}$, where α is the dissociation fraction, D the diameter of the sphere, u the velocity; and the subscripts "∞" and "s" means the corresponding quantities at freestream and

immediately behind the shock, respectively. Depending on the value of Ω, the flow can be categorized into nearly frozen flow ($\Omega \ll 1$), nearly equilibrium flow ($\Omega \gg 1$), and non-equilibrium flow (otherwise). The distance between the bow shock and the stagnation point of the nose was referred to as the Shock Stand-off Distance (SSD). The SSD is much smaller than the size of the tested model, and hence experimental measurement admits large errors. Generally speaking, if there is no significant dissociation in the free stream, a larger free stream kinetic energy leads a smaller SSD, due to a higher level of vibrational excitation and chemical dissociation. But an increased SSD is observed in high enthalpy shock tunnels under the same free stream velocity and this phenomenon is attributed to the inevitable free stream dissociation in such facilities.[2,3] In order to understand the physics behind, it is crucial to explore the effects of the important flow parameters through theoretical analysis. Olivier et al.[2] first gave an

ELSEVIER | **Production and hosting by Elsevier**

estimation of the effect of free stream dissociation on SSD, but no quantitative solution was provided.

For frozen flows, Lobb[4] performed extensive experiments on the SSD for spheres of various diameters using a schlieren photography technique and derived the following correlation

$$\frac{\Delta}{D} = L \frac{\rho_\infty}{\rho_s}$$

where Δ is the SSD, ρ density, L a constant with a value of 0.41 for spheres. For dissociating flows, the accuracy of Lobb's correlation is significantly degraded.[5,6]

Wen and Hornung[5] proposed an analytic correlation between generalized dimensionless SSD $\left(\tilde{\Delta} \equiv \frac{\Delta}{D} \cdot \frac{\rho_s}{\rho_\infty} \right)$ and the generalized reaction rate parameter $\left(\tilde{\Omega} \equiv \left(\frac{d\rho}{dt} \right)_s \frac{D}{\rho_s u_\infty} \right)$, which comprises two branches, namely a frozen-side and an equilibrium-side. The frozen-side solution is given by

$$\tilde{\Delta} = \frac{1}{\tilde{\Omega}} \left(-1 + \sqrt{1 + 2L\tilde{\Omega}} \right)$$

which implies the SSD is independent of all parameters other than L. Meanwhile, the equilibrium-side solution is given by

$$\tilde{\Delta} = \frac{\rho_s}{\rho_e} \left[L + \frac{1}{2\tilde{\Omega}} \left(\frac{\rho_e}{\rho_s} - 1 \right)^2 \right]$$

which implies the importance of the density ratio ρ_s/ρ_e (note that the subscript "e" denotes the corresponding quantities at fully equilibrium states). This simple correlation is well validated by experiments,[5,7] CFD results[8,9] and a quasi-one-dimensional model.[10] However, it relies on the semi-empirical parameter L measured by experiments, and therefore cannot completely reveal the embedded physics.

Based on a differential analysis of the governing conservation equations, Olivier[11] proposed the following analytic solution for the SSD in frozen and equilibrium flows:

$$\tilde{\Delta} = \left\{ \frac{\rho_s}{\rho_\infty} \sqrt{\frac{1}{4} \left[1 + \left(\frac{\partial \tilde{u}}{\partial \phi} \right)_b \right]^2 - \frac{1}{3} \cdot \frac{\rho_s}{\rho_b} \cdot \frac{\rho_\infty}{\rho_s} \left[1 + 2 \left(\frac{\partial \tilde{u}}{\partial \phi} \right)_b \right]} \right.$$
$$\left. - \frac{1}{2} \left[1 + \left(\frac{\partial \tilde{u}}{\partial \phi} \right)_b \right] \frac{\rho_s}{\rho_\infty} + \frac{\rho_s}{\rho_b} \right\} \left[\frac{4}{3} + \frac{2}{3} \left(\frac{\partial \tilde{u}}{\partial \phi} \right)_b - 2 \frac{\rho_s}{\rho_b} \cdot \frac{\rho_\infty}{\rho_s} \right]^{-1}$$

where $\frac{\partial \tilde{u}}{\partial \phi}$ is the dimensionless tangential velocity gradient and the subscript "b" represents corresponding values at the stagnation point (body). For frozen air flows, i.e., $\rho_s/\rho_b = 1$ and $\rho_s/\rho_\infty = 6$, the Olivier's analytic solution has a value of $\tilde{\Delta} = 0.4$, and is thus in good agreement with the solution obtained from Lobb's correlation. Significantly, Olivier's model shows that the parameter L is not constant but depends on the gas properties. Nevertheless, since non-equilibrium processes increase the complexity of the conservation equations to such an extent that even for a quasi-one-dimensional approach, analytic solutions cannot be obtained for the whole non-equilibrium flow regimes.[12]

In view of the discussions above, the present study has two aims: (A) to derive a comprehensive analytic solution for the whole non-equilibrium flow regime without using the semi-empirical parameter L; (B) to investigate the effect of two fundamental flow parameters, namely the freestream kinetic energy, and the freestream dissociating level, on the SSD using a simple Ideal Dissociating Gas (IDG) model.[13,14]

2. Analytic solution for shock stand-off distance

Consider the control volume ΔV in the stagnation region between the shock and the body, as shown in Fig. 1. The rate at which mass enters the control volume from the left-hand side is equal to $\rho_\infty u_\infty b$ or $\rho_\infty u_\infty b^2$, depending on whether the flow is two-dimensional or axisymmetric, respectively. Meanwhile, the rate at which mass leaves the control volume through the right-hand side is equal to

$$\int_R^{R+\Delta} \rho u_\tau \, dr \quad \text{or} \quad 2 \int_R^{R+\Delta} \rho u_\tau r \sin \phi \, dr$$

where u_τ is the tangential velocity (i.e., the component of velocity normal to the ray from the center of curvature), R is the radius of the sphere and dr is the differential element of the radius. Consequently, the mass balance is given as

$$\rho_\infty u_\infty b = \int_R^{R+\Delta} \rho u_\tau \, dr \tag{1}$$

and

$$\rho_\infty u_\infty b^2 = 2 \int_R^{R+\Delta} \rho u_\tau r \sin \phi \, dr \tag{2}$$

for two-dimensional and axisymmetric flows, respectively. The integral terms in Eqs. (1) and (2) can be approximated using the average value, i.e.,

$$\int_R^{R+\Delta} \rho u_\tau \, dr = \overline{\rho u_\tau} \Delta \tag{3}$$

and

$$\int_R^{R+\Delta} \rho u_\tau r \sin \phi \, dr = \overline{\rho u_\tau} \frac{1}{2} (2R\Delta + \Delta^2) \sin \phi \tag{4}$$

Furthermore, let only the flow region very close to the stagnation streamline be considered. Therefore, the following approximations can be applied:

$$b \approx (R + \Delta) \tan \phi, \quad \sin \phi \approx \tan \phi \approx \phi, \quad u_\tau = \phi \frac{\partial u_\tau}{\partial \phi} \tag{5}$$

As a result, the solution method is restricted to this area since only the stand-off distance at the stagnation point is of interest and Eqs. (1) and (2) can be re-written as
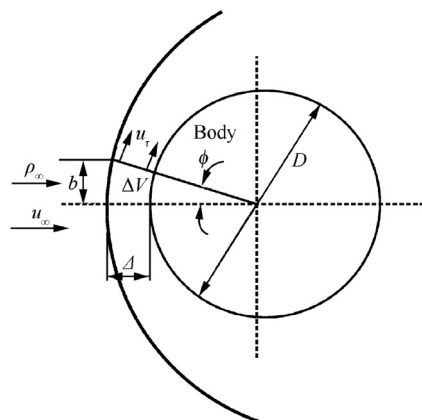

Fig. 1 Schematic of control volume and associated notations.

$$\chi\left(\frac{\varDelta}{R}\right) - 1 = 0 \tag{6}$$

and

$$\chi\left(\frac{\varDelta}{R}\right)^2 + 2\chi\left(\frac{\varDelta}{R}\right) - 1 = 0 \tag{7}$$

with solutions

$$\bar{\varDelta} \equiv \frac{\varDelta}{R} = \frac{1}{\chi} \tag{8}$$

and

$$\bar{\varDelta} \equiv \frac{\varDelta}{R} = \frac{-2\chi + \sqrt{(2\chi + 1)^2 - 1}}{2\chi} \tag{9}$$

respectively, where

$$\chi = \overline{\rho\frac{\partial u_\tau}{\partial \phi}} \Big/ (\rho_\infty u_\infty) - 1 \tag{10}$$

Since $\frac{\partial u_\tau}{\partial \phi}/u_\infty$ is $O(1)$ (this point can be further verified later) and ρ/ρ_∞ is very large for hypersonic flows, it follows that

$$\sqrt{(2\chi + 1)^2 - 1} \approx 2\chi + 1 \tag{11}$$

Substituting Eq. (11) into Eq. (9) yields the following simple solution for SSD in axisymmetric flow:

$$\bar{\varDelta} \approx \frac{1}{2\chi} \tag{12}$$

Obviously, the parameter χ is the measurement of the product of density and the tangential velocity gradient. Eqs. (8) and (12) imply that the dimensionless SSD is inversely proportional to χ. The above derivations using integral analyses are obviously more succinct than Olivier's correlation derived from the differential analyses. Comparing Eqs. (8) and (12), the SSD for a cylinder exhibits the same qualitative behavior as that for a sphere. However, the tangential velocity gradient for a cylinder is smaller than that for a sphere,[12] and thus the SSD is more than twice that of a sphere. The following derivation will be focused on the SSD for spheres.

To determine the SSD for spheres using Eq. (9) or (12), the tangential velocity gradient must be solved. At the point immediately behind the shock, the velocity gradient can be determined from the conserved tangential velocity component across the shock, i.e.,

$$\left(\frac{\partial u_\tau}{\partial \phi}\right)_s = u_\infty \cos \phi \approx u_\infty \tag{13}$$

Meanwhile, from the momentum equation in the tangential direction at the body, we have[15]

$$\rho_b u_\tau \frac{\partial u_\tau}{\partial \phi} + \frac{\partial p_b}{\partial \phi} = 0 \tag{14}$$

where p is the pressure. Utilizing the approximation of velocity in Eq. (5) and assuming a Newtonian pressure distribution over the surface, i.e., $p_b - p_\infty = \rho_\infty u_\infty^2 \cos^2 \phi$, Eq. (14) can be written as

$$\rho_b \phi \left(\frac{\partial u_\tau}{\partial \phi}\right)^2 - 2\rho_\infty u_\infty^2 \cos \phi \sin \phi = 0 \tag{15}$$

From Eqs. (5) and (15), we can get the solution of tangential velocity gradient as

$$\left(\frac{\partial u_\tau}{\partial \phi}\right)_b = u_\infty \sqrt{\frac{2\rho_\infty}{\rho_b}} \tag{16}$$

Following Olivier,[11] an assumption is made here that the tangential velocity gradient profile varies linearly with distance between the body and shock wave. For frozen flows and fully equilibrium flows, the density in the stagnant region can be treated constant and the expression of χ can be simply written as

$$\chi = \frac{\rho_{avg}}{2\rho_\infty}\left(1 + \sqrt{2\frac{\rho_\infty}{\rho_s}\cdot\frac{\rho_s}{\rho_b}}\right) - 1 \tag{17}$$

where ρ_{avg} is the average density along the stagnant line which is equal to ρ_s and ρ_e for frozen flows and fully equilibrium flows, respectively. For hypervelocity frozen air flows, $\rho_s/\rho_b = 1$ and $\rho_s/\rho_\infty = 6$. Hence, Eqs. (9) and (12) yield SSDs of $\tilde{\varDelta} = 0.38$ and 0.40, respectively. Both solutions are in good agreement with the results obtained from Lobb's approximation and Olivier's model, i.e., 0.41 and 0.40, respectively. The SSD of $\tilde{\varDelta} = 0.38$ derived by the more rigorous Eq. (9) is slightly less than Lobb's approximation and Olivier's model. Nevertheless, it is interesting to note that for the frozen nitrogen flows, Hornung[1] derived a value for SSD of $\tilde{\varDelta} = 0.39$ which is also slightly less than that given by Lobb's approximation. Moreover, $\tilde{\varDelta}$ calculated from Eqs. (9) and (12) has only a weak dependence on ρ_s/ρ_∞ for hypersonic frozen flows which is consistent with that first reported by Olivier.[11] When freestream Mach number $Ma_\infty \to \infty$, the value of ρ_s/ρ_∞ depends on the value of γ (adiabatic index). In order to compare the present model with Oliver's model[11], the dimensionless SSDs for different gases are listed in Table 1. It is observed that the present model is not as sensitive to ρ_s/ρ_∞ as Olivier's model. For large value of ρ_s/ρ_∞, the present theory agrees well with Olivier's theory. But for the monoatomic gas flow ($\gamma = 5/3$, $\rho_s/\rho_\infty = 4.0$), the difference between the two theories is more obvious.

The values of ρ/ρ_∞ for non-equilibrium and fully equilibrium flows are larger than that for frozen flows, and the solutions obtained from Eqs. (9) and (12), respectively, tend to converge. Therefore, only the concise correlation Eq. (12) is employed in the following calculations. Eqs. (12) and (17) show that the density ratio ρ_s/ρ_b plays an important role in determining the SSD in non-equilibrium dissociating flows, which is consistent with the observations of Wen and Hornung[5] and Olivier,[11] respectively.

Table 1   Dimensionless SSD ($\tilde{\varDelta}$) of frozen flows for gases with different values of ρ_s/ρ_∞.

Model	Dimensionless SSD ($\tilde{\varDelta}$)		
	CO_2 ($\rho_s/\rho_\infty = 7.67$)	Monoatomic gas ($\rho_s/\rho_\infty = 4.0$)	Ideal dissociating gas ($\rho_s/\rho_\infty = 7.0$)
Present, Eq. (9)	0.38	0.38	0.38
Present, Eq. (12)	0.40	0.41	0.40
Olivier[11]	0.38	0.44	0.39

Table 2 Dimensionless SSD ($\tilde{\Delta}$) of fully equilibrium flows for gases with different values of ρ_s/ρ_b provided with $\rho_s/\rho_\infty = 6.0$.

Model	Dimensionless SSD ($\tilde{\Delta}$)					
	$\rho_s/\rho_b = 0.4$	$\rho_s/\rho_b = 0.5$	$\rho_s/\rho_b = 0.6$	$\rho_s/\rho_b = 0.7$	$\rho_s/\rho_b = 0.8$	$\rho_s/\rho_b = 0.9$
Present, Eq. (12)	0.162	0.201	0.241	0.280	0.320	0.361
Wen and Hornung[5]	0.164	0.205	0.246	0.287	0.328	0.369
Olivier[11]	0.164	0.203	0.241	0.280	0.319	0.359

Table 2 compares the values of the dimensionless SSD, $\tilde{\Delta} \equiv \frac{\Delta}{D} \cdot \frac{\rho_s}{\rho_\infty}$, obtained by Eqs. (12), Wen and Hornung's theory[5] and Oliver's theory,[11] respectively, given various values of the density ratio ρ_s/ρ_b ranging from 0.4 to 0.9 provided with $\rho_s/\rho_\infty = 6.0$. It is observed that a good agreement exists between the three sets of results.

3. Correlation between shock stand-off distance and reaction rate parameter

Eqs. (10) and (12) imply that if ρ_s/ρ_∞ is known, the SSD can be determined from the average value of $\overline{\rho \frac{\partial u_\tau}{\partial \phi}}/(\rho_\infty u_\infty)$. Note that, the tangential velocity gradient is already solved in the last section. On the other hand, the generalized reaction rate parameter, i.e., $\tilde{\Omega} \equiv \left(\frac{d\rho}{dt}\right)_s \frac{D}{\rho_s u_\infty}$, can be rewritten as

$$\tilde{\Omega} = \left(\frac{d\rho}{dy}\right)_s \frac{Du_s}{\rho_s u_\infty} \tag{18}$$

where y denotes the horizontal direction. In other words, the reaction rate parameter is governed by the spatial gradient of the density immediately behind the shock. As a result, the SSD can be correlated with the generalized reaction rate parameter by means of the density profile between the shock and the body.

3.1. A correlation using exponential density profile

Wen and Hornung[5] used a piecewise linear function to approximate the density profile. They pointed out that the use of a piecewise linear function to approximate the density profile between the shock and the body results in an overestimation of the average density, and hence an underestimation of the SSD. This error can be reduced by replacing the piecewise linear function with the following exponential function:

$$\rho = \rho_e - (\rho_e - \rho_s)e^{-\lambda\frac{y}{\Delta}} \quad 0 \leqslant y \leqslant \Delta \tag{19}$$

where λ ranges from zero to infinity. As shown, Eq. (19) is a monotonic function for ρ with respect to λ and the density reduces to ρ_s (frozen flows) and ρ_e (fully equilibrium flows) when $\lambda = 0$ and ∞, respectively. In other words, every flow regime within the range of the frozen flow to the fully equilibrium flow is represented by a specific value of λ between 0 and ∞.

Using Eq. (19), the density ratio between the shock and the body and the product of density and tangential velocity gradient and can be given as

$$\frac{\rho_b}{\rho_s} = \frac{\rho_e}{\rho_s} - \left(\frac{\rho_e}{\rho_s} - 1\right)e^{-\lambda} \tag{20}$$

and

$$\overline{\rho\frac{\partial u_\tau}{\partial \phi}}\Big/(\rho_\infty u_\infty) = \left(1 - \frac{\rho_e}{\rho_s}\right)\frac{\rho_s}{\rho_\infty}$$
$$\cdot\sqrt{2\frac{\rho_\infty}{\rho_s}\Big/\left[\frac{\rho_e}{\rho_s} - \left(\frac{\rho_e}{\rho_s} - 1\right)e^{-\lambda}\right]}\left(\frac{1 - e^{-\lambda}}{\lambda^2} - \frac{e^{-\lambda}}{\lambda}\right)$$
$$+ \left(1 - \frac{\rho_e}{\rho_s}\right)\frac{\rho_s}{\rho_\infty}\left(\frac{1}{\lambda} + \frac{e^{-\lambda} - 1}{\lambda^2}\right) + \frac{1}{2}$$
$$\cdot\frac{\rho_e}{\rho_\infty}\left(1 + \sqrt{2\frac{\rho_\infty}{\rho_s}\Big/\left[\frac{\rho_e}{\rho_s} - \left(\frac{\rho_e}{\rho_s} - 1\right)e^{-\lambda}\right]}\right) \tag{21}$$

respectively. From Eq. (19), we can easily verify that

$$\lambda = \left(\frac{d\rho}{dy}\right)_s \frac{\Delta}{\rho_e - \rho_s} \tag{22}$$

which represents the dimensionless density gradient right after the shock. Clearly, an explicit correlation is no longer possible. But the following uniform implicit correlation can be derived

$$\begin{cases} \frac{1}{\tilde{\Delta}} = 4\left(1 - \frac{\rho_e}{\rho_s}\right)\sqrt{2\frac{\rho_\infty}{\rho_s}\Big/\left[\frac{\rho_e}{\rho_s} - \left(\frac{\rho_e}{\rho_s} - 1\right)e^{-\lambda}\right]}\left(\frac{1-e^{-\lambda}}{\lambda^2} - \frac{e^{-\lambda}}{\lambda}\right) \\ +4\left(1 - \frac{\rho_e}{\rho_s}\right)\left(\frac{1}{\lambda} + \frac{e^{-\lambda} - 1}{\lambda^2}\right) + 2\frac{\rho_e}{\rho_s}\left(1 + \sqrt{2\frac{\rho_\infty}{\rho_s}\Big/\left[\frac{\rho_e}{\rho_s} - \left(\frac{\rho_e}{\rho_s} - 1\right)e^{-\lambda}\right]}\right) - 4\frac{\rho_\infty}{\rho_s} \\ \lambda = \tilde{\Delta}\tilde{\Omega}\Big/\left(\frac{\rho_e}{\rho_s} - 1\right) \end{cases} \tag{23}$$

3.2. Comparison and discussion

Eq. (23) shows that the correlation between $\tilde{\Delta}$ and $\tilde{\Omega}$ depends on the values of ρ_s/ρ_∞ and ρ_s/ρ_e, respectively. Fig. 2 shows the variation of $\tilde{\Delta}$ with $\tilde{\Omega}$ as a function of ρ_s/ρ_e given a constant $\rho_s/\rho_\infty = 6$. Notably, the physical significance of $\tilde{\Omega}$ is the ratio between the energy absorption rate by chemistry and the input rate of free stream kinetic energy.[5] For small $\tilde{\Omega}$, no chemical reaction occurs in the flow and thus the scaled SSD remains constant. However, as $\tilde{\Omega}$ increases, the amount of energy absorbed by vibrational excitations and chemical reactions also increases. As a result, the average density increases, while $\tilde{\Delta}$ decreases. As expected for the non-equilibrium regime, using exponential density approach gives a higher value of SSD than Wen and Hornung's correlation[5] using linear density approach.

As described above, the scaled SSD is dependent on ρ_s/ρ_∞ and ρ_s/ρ_e. For an ideal dissociating gas with no freestream dissociation, ρ_s/ρ_∞ is equal to 7. For CO_2 with $Ma_\infty \to \infty$, ρ_s/ρ_∞ is equal to 7.67. Fig. 3 plots $\tilde{\Delta}$ and $\bar{\Delta}$ versus $\tilde{\Omega}$ for different val-
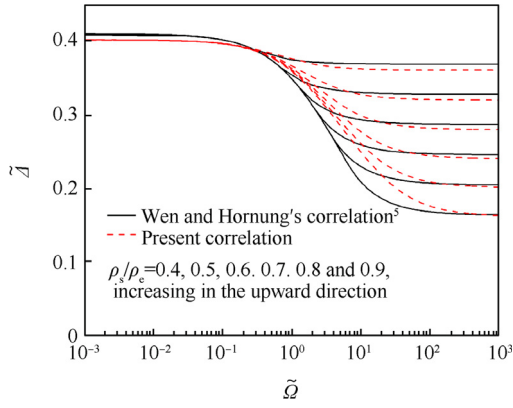
Fig. 2   Scaled SSD $\tilde{\Delta}$ as function of reaction rate parameter $\tilde{\Omega}$ given $\rho_s/\rho_\infty = 6$.
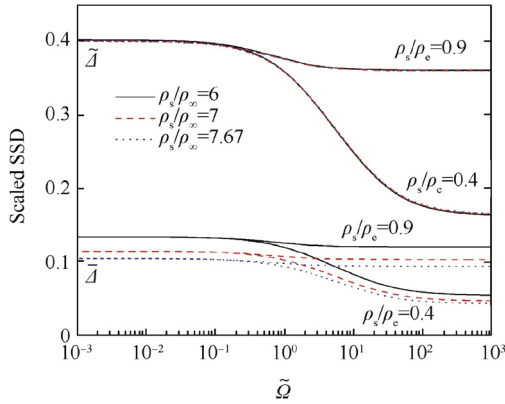

Fig. 3   Effect of ρ_s/ρ_∞ on scaled SSD $\tilde{\Delta}$ and $\bar{\Delta}$ for different values of ρ_s/ρ_e.

4. Analytic solution for stand-off distance of nitrogen flows using ideal dissociating gas model

4.1. Basic equations

The analytic solutions derived in the previous section are not restricted to any specific gas model, and show that $\tilde{\Delta}$ is determined by both ρ_s/ρ_∞ and ρ_s/ρ_e. However, in experimental and simulation studies, the freestream condition is usually expressed in terms of freestream values of ρ_∞, u_∞, T_∞ and α_∞ (T_∞ is the freestream temperature). Wen and Hornung[5] qualitatively described the effect of free stream kinetic energy on the scaled SSD $\tilde{\Delta}$. However, no quantitative relation was derived. Thus, in the present study, the simple IDG model is used to quantify the effects of the main flow parameters on

the scaled SSD analytically, for the illustrative case of nitrogen flows. The analysis is also suitable for other pure dissociating diatomic gases and can be extended to multi-component gases by using the approach proposed by Olivier and Gartz.[16]

The boundary conditions on the shock wave can be determined by enforcing the conservation of energy, momentum, mass and dissociation fraction across the shock, i.e.,

$$\begin{cases} h_\infty + \frac{1}{2}u_\infty^2 = h_s + \frac{1}{2}u_s^2 \\ p_\infty + \rho_\infty u_\infty^2 = p_s + \rho_s u_s^2 \\ \rho_\infty u_\infty = \rho_s u_s \\ \alpha_\infty = \alpha_s \end{cases} \tag{24}$$

where h is the specific enthalpy. In general, the equation of state for a mixture of molecular and atomic nitrogen is given as

$$p = \rho(1+\alpha)\frac{R_u}{M}T \tag{25}$$

where M is the molecular weight of N_2, T is the temperature and R_u is the universal gas constant. Meanwhile, the specific enthalpy for an IDG is given by

$$h = \frac{4+\alpha}{1+\alpha} \cdot \frac{p}{\rho} + \alpha\frac{R_u\theta_d}{M} \tag{26}$$

where θ_d is the characteristic dissociating temperature for nitrogen and has a value of 113200 K. The boundary condition for h at the shock is then expressed as follows:

$$\frac{Mh_s}{R_u\theta_d} = (4+\alpha_\infty)\frac{T_\infty}{\theta_d} + \frac{Mu_\infty^2}{2R_u\theta_d} + \alpha_\infty \tag{27}$$

where the velocity component normal to the shock is neglected in the shock layer.

Utilizing the state equation and the definition of enthalpy, the temperature immediately behind the shock can be obtained from Eq. (27) with $\alpha_s = \alpha_\infty$ as

$$\frac{T_s}{\theta_d} = \frac{T_\infty}{\theta_d} + \frac{\mu}{4+\alpha_\infty} \tag{28}$$

where $\mu \equiv \frac{Mu_\infty^2}{2R_u\theta_d}$ is the dimensionless kinetic energy parameter. For hypersonic flows, the approximation $\frac{p_s}{\rho_\infty u_\infty^2} = 1$ is widely adopted. Eqs. (25) and (28) thus yield the following expression for the density:

$$\frac{\rho_s}{\rho_\infty} = \frac{2\mu}{1+\alpha_\infty} \cdot \frac{\theta_d}{T_s} \tag{29}$$

From equilibrium theory of Lighthill,[14] the equilibrium dissociation fraction α_e can be determined as

$$\frac{\alpha_e^2}{1-\alpha_e} = \frac{\rho_d}{\rho_e}e^{-\theta_d/T_e} \tag{30}$$

Here, ρ_d is the characteristic dissociation density, and was reported by Lighthill[14] to have a value of 1.3×10^5 kg/m^3 for nitrogen.

To solve α_e, ρ_e and T_e from Eq. (30), two more equations are required. The first equation can be derived by enforcing the conservation of the total enthalpy, i.e.,

$$\frac{T_e}{\theta_d} = \frac{(4+\alpha_\infty)\frac{T_\infty}{\theta_d} + (\alpha_\infty - \alpha_e) + \mu}{4+\alpha_e} \tag{31}$$

Meanwhile, the second equation can be derived directly from the state equation, i.e.,

---

ues of ρ_s/ρ_∞. It is seen that while $\tilde{\Delta}$ has a very weak dependence on ρ_s/ρ_∞, $\bar{\Delta}$ has a strong dependence on ρ_s/ρ_∞. For a constant $\tilde{\Omega}$, when ρ_s/ρ_∞ increases, $\bar{\Delta}$ decrease significantly, but $\tilde{\Delta}$ almost remains the same. In other words, $\tilde{\Delta}$ is a more universal dimensionless parameter than $\bar{\Delta}$ in estimating the SSD.

$$\frac{\rho_e}{\rho_\infty} = \frac{2\mu}{(1 + \alpha_e)\frac{T_e}{\theta_d}} \quad (32)$$

From Eqs. (30)–(32), α_e, ρ_e and T_e can all be solved. Although explicit solutions are impossible, they nevertheless demonstrate the roles of the dimensionless parameters T_∞/θ_d, ρ_d/ρ_∞, μ and α_∞ in determining the shock stand-off position. Notably, T_∞ and α_∞ can be very different from the real flight conditions in a free-piston shock tunnels.

4.2. Effects of μ and α_∞ on SSD

In the following discussions, ρ_s/ρ_∞ and ρ_s/ρ_e are derived from (29) and (30)–(32), respectively. Then they are used as the inputs of the correlation of $\tilde{\Delta}$ and $\tilde{\Omega}$.

Fig. 4 shows the variation of $\tilde{\Delta}$ with $\tilde{\Omega}$ as a function of μ given $\frac{\rho_d}{\rho_\infty} = 10^6$, $\frac{T_\infty}{\theta_d} = 2.6 \times 10^{-3}$ and $\alpha_\infty = 0$. It is seen that the scaled SSD $\tilde{\Delta}$ depends very weakly on μ on the frozen side ($\tilde{\Omega} \ll 1$). However, $\tilde{\Delta}$ reduces significantly with increasing μ on the equilibrium side ($\tilde{\Omega} \gg 1$). When $\mu = 0.15$ ($u_\infty = 3175$ m/s), $\tilde{\Delta}$ on the frozen side and equilibrium side are almost equal. It indicates that when the free stream velocity of nitrogen flow is smaller than 3175 m/s, the dissociating reactions in the flow can be neglected. Notably, although when the freestream velocity decreases to around 3.2 km/s, the dissociation is very weak, the vibrational excitation may decrease a few percentages of $\tilde{\Delta}$ (see Houwing et al.[17]). When μ increases to 1 and beyond, the corresponding $\tilde{\Delta}$-$\tilde{\Omega}$ curves are approximately superimposed. From the physics perspective, for nearly frozen flow, no chemical reaction occurs to increase the average density. As a consequence, $\tilde{\Delta}$ is effectively independent of $\tilde{\Omega}$ and remains almost constant. For non-equilibrium and nearly equilibrium flows, the amount of energy absorbed by chemical dissociation increases with increasing the freestream kinetic energy parameter μ. As a result, ρ_e/ρ_s increases and $\tilde{\Delta}$ decreases. For the particular case of $\mu = 1.0$, the freestream kinetic energy is equal to the specific dissociation energy of the gas and the amount of energy absorbed by chemical dissociation reaches to the upper limit. Consequently, ρ_e/ρ_s no longer increases even when μ increases, and $\tilde{\Delta}$ reaches its minimum value. Overall, Fig. 4 infers that the change in the scaled
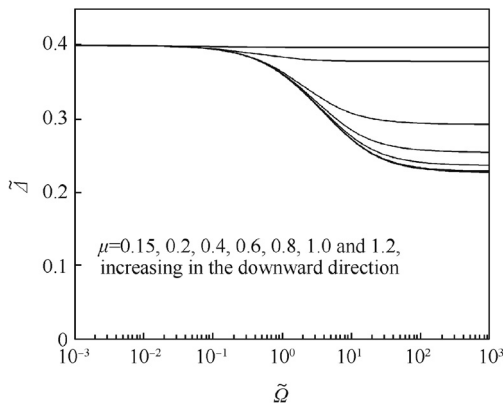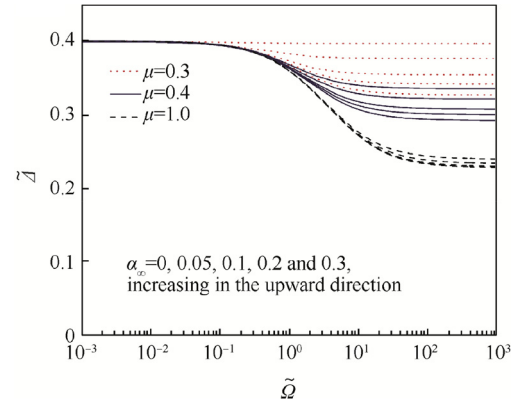

Fig. 5 Effect of freestream dissociation level α_∞ on scaled SSD $\left(\frac{\rho_d}{\rho_\infty} = 10^6, \frac{T_\infty}{\theta_d} = 2.6 \times 10^{-3}\right)$.

SSD $\tilde{\Delta}$ is due primarily to the energy absorption caused by chemical reactions.

The solution shown in Fig. 4 is based on $\alpha_\infty = 0$ which is the case for the ballistic range experiment.[18] However, in the high enthalpy free-piston shock tunnel tests,[19,20] the freestream dissociation level is not zero anymore. Using the IDG model, we can quantitatively estimate the influence of freestream dissociation level on the SSD. Belouaggadia et al.[12] investigated the effect of the freestream dissociation level, α_∞, on the shock stand-off distance for the cases of frozen flows and fully equilibrium flows. In the present study, the effect of α_∞ on $\tilde{\Delta}$ is investigated over the entire non-equilibrium flow regime. As shown in Fig. 5, α_∞ has only a weak effect on $\tilde{\Delta}$ for the case of nearly frozen flows, which is the case presented by Belouaggadia, et al..[12] In addition, it is seen that $\tilde{\Delta}$ increases significantly with increasing α_∞ for moderate values of μ, but is insensitive to α_∞ at larger values of μ. When $\alpha_\infty = 0.3$ and $\mu = 0.4$, the SSD is even larger than that of $\alpha_\infty = 0$ and $\mu = 0.3$. It means the two opposite acting effects, decrease of the SSD by high freestream kinetic effects and increase of the SSD by free stream dissociation, may even cancel each other.[2] This finding is reasonable since in higher α_∞ flows, dissociating chemical reactions occur less readily due to the absence of educts, and hence the density change is less obvious than that in the case of flows with low α_∞. When μ is sufficiently large (e.g., $\mu = 1$), dissociation anyway takes place easily, for α_∞ ranging from 0 to 0.3, and hence no change of $\tilde{\Delta}$-$\tilde{\Omega}$ curve occurs. In general, the curves presented in Fig. 5 imply that the effects of possible freestream dissociation in high-enthalpy wind tunnels must be considered, particularly for the case of moderate μ.

5. Conclusions

A comprehensive analytical solution has been derived to calculate the SSD and to correlate the SSD of hypervelocity non-equilibrium flows with the average density between the shock and the body without the need for any specific gas model or empirical parameters. Furthermore, using an exponential function to approach the density distribution between the shock and the body, the scaled SSD $\tilde{\Delta}$ has been correlated with the

Fig. 4 Effect of freesteam kinetic parameter μ on scaled SSD $\left(\frac{\rho_d}{\rho_\infty} = 10^6, \frac{T_\infty}{\theta_d} = 2.6 \times 10^{-3}, \alpha_\infty = 0\right)$.

reaction rate parameter $\tilde{\Omega}$. In general, the results have shown that:

(1) the correlation curve is strongly dependent on ρ_s/ρ_e, but is only weakly dependent on ρ_s/ρ_∞.
(2) $\tilde{\Delta}$ is a more universal dimensionless parameter than $\bar{\Delta}$ in estimating the SSD. The effects on the SSD of the free-stream kinetic energy parameter, μ, and the freestream dissociation level, α_∞, have been investigated using a simple ideal dissociating gas (IDG) model. The results imply an underlying physical mechanism which can be described as the reduction of the scaled SSD $\tilde{\Delta}$ is due to the greater energy absorption caused by chemical reactions. The effects of possible freestream dissociation in high-enthalpy wind tunnels must be considered; particularly for the case of moderate μ.

Acknowledgements

References

1. Hornung HG. Non-equilibrium dissociating nitrogen flow over spheres and circular cylinders. *J Fluid Mech* 1972;**53**:149–76.
2. Olivier H, Walpot L, Merrifield J, Molina R. On the phenomenon of the shock stand-off distance in hypersonic, high enthalpy facilities. In: Jiang Z, editor. *Proceedings of the first international conference on high temperature gas dynamics*; 2012 Oct 15–17; Beijing, China. Beijing: Institute of Mechanics, Chinese Academy of Sciences; 2012. p. 92–100.
3. Hashimoto T, Komuro T, Sato K, Itoh K. Experimental investigation of shock stand-off distance on spheres in hypersonic nozzle flows. In: Hannemann K, Seiler F, editors. *Shock waves*. Heidelberg: Springer; 2009. p. 961–6.
4. Lobb RK. Experimental measurement of shock detachment distance on spheres fired in air at hypervelocities. In: Nelson WC, editor. *The high temperature aspects of hypersonic flow*. Oxford: Pergamon Press; 1964. p. 519–27.
5. Wen CY, Hornung HG. Non-equilibrium dissociating flow over spheres. *J Fluid Mech* 1995;**299**:389–405.
6. Nonaka S, Mizuno H, Takayama K, Park C. Measurement of shock standoff distance for sphere in ballistic range. *J Thermophys Heat Transf* 2000;**14**(2):225–9.
7. Sarma GSR. Physico-chemical modelling in hypersonic flow simulation. *Prog Aerosp Sci* 2000;**36**(3–4):281–349.
8. Gerdroodbary MB, Hosseinalipour SM. Numerical simulation of hypersonic flow over highly blunted cones with spike. *Acta Astronaut* 2010;**67**(1–2):180–93.
9. Shen H, Wen CY, Massimi HS. Application of CE/SE method to study hypersonic non-equilibrium flows over spheres. Reston: AIAA; 2014. Report No.: AIAA-2014-2509.
10. Chen S, Sun Q. A quasi-one-dimensional model for hypersonic reactive flow along the stagnation streamline. *Chin J Aeronaut* 2016;**29**(6):1517–26.
11. Olivier H. A theoretical model for the shock stand-off distance in frozen and equilibrium flow. *J Fluid Mech* 2000;**413**:345–53.
12. Belouaggadia N, Olivier H, Brun R. Numerical and theoretical study of the shock stand-off distance in non-equilibrium flows. *J Fluid Mech* 2008;**607**:167–97.
13. Freeman NC. Non-equilibrium flow of an ideal dissociating gas. *J Fluid Mech* 1958;**4**(4):407–25.
14. Lighthill MJ. Dynamics of a dissociating gas—Part I: Equilibrium flow. *J Fluid Mech* 1957;**2**(1):1–32.
15. Anderson JD. *Hypersonic and high-temperature gas dynamics*. 2nd ed. Reston: AIAA; 2006. p. 311.
16. Olivier H, Gartz R. Extension of Lighthill's gas model for multicomponent air. 5th European conference for aeronautics and space sciences; 2013. p. 1–8.
17. Houwing AFP, Nonaka S, Mizuno H, Takayama K. Effects of vibrational relaxation on now shock standoff distance for nonequilibrium flows. *AIAA J* 2000;**38**(9):1760–3.
18. Nonaka S, Mizuno H, Takayama K. Ballistic range measurement of shock shapes in intermediate hypersonic range. Reston: AIAA; 1999. Report No.: AIAA-1999-1025.
19. Wen CY. Hypervelocity flow over spheres [dissertation]. Pasadena: California Institute of Technology; 1994. 142–58.
20. Belouaggadia N, Hashimoto T, Nonaka S, Takayama K, Brun R. Shock detachment distance on blunt bodies in nonequilibrium flow. *AIAA J* 2007;**45**(6):1424–9.